2002

Application Of CFD Models To Two-Phase Flow In Refrigerant Distributors

G. Li
Purdue University

S. H. Frankel
Purdue University

J. E. Braun
Purdue University

E. A. Groll
Purdue University

APPLICATION OF CFD MODELS TO TWO-PHASE FLOW IN REFRIGERANT DISTRIBUTORS

Gang Li, Steven Frankel, James E. Braun*, and Eckhard A. Groll

Purdue University, 1077 Ray W. Herrick Laboratories
West Lafayette, IN 47907, USA
*Author for Correspondence E-Mail: jbraun@ecn.purdue.edu

ABSTRACT

The goal of the work described in this paper was to identify an appropriate CFD model for refrigerant distributors that could be used to develop improved designs. There appears to have been no previous work applying CFD to two-phase flow in refrigerant distributors. As a first step in evaluating the applicability of CFD to two-phase flow in refrigerant distributors, results of predictions from two commonly available codes, FLUENT and PHOENICS, were compared with experimental results available in the literature for two-phase flow distribution with air and water as working fluids. FLUENT 5.5 failed to predict the experimental data available, whereas PHOENICS predictions were in close agreement with the measurements in all cases. However, for a typical refrigerant distributor geometry and set of operating conditions, predictions of two-phase distribution and separation were quite similar for FLUENT 5.5 and PHOENICS. As a result, FLUENT is applicable for studying improved refrigerant distributor designs and was used for this purpose as described in a companion paper by Li et. al. (2002).

Introduction

Figure 1 depicts a vapor compression cycle with a refrigerant flow distributor. Following the expansion device, two-phase refrigerant enters the distribution device and is divided into multiple flow circuits that feed the evaporator. Ideally, the distributor should provide equal mass flow rates and qualities to each flow circuit of the evaporator. However, it is difficult to design and manufacture a refrigerant flow distributor that will split a two-phase refrigerant mixture evenly between different outlet branches. The distribution of liquid and vapor phases is very sensitive to the conditions and orientation of the flow entering the distributor and to the orientation of the distributor.

The design of refrigerant flow distributors is typically a trial-and-error process. Modifications are proposed, a prototype is built, and the device is tested. An alternative approach, described in this paper, is to use CFD modeling for the problem of flow and phase distribution in refrigerant distributors. Often, a removable orifice is located within the base of the distributor. The refrigerant flows through the orifice, expands from a liquid to a two-phase refrigerant mixture into the base of the distributor and then branches into the different (four shown in Figure 1) feeder tubes leading to the evaporator. A vertically installed distributor with no manufacturing defects and with symmetrically oriented branches would produce even flow and phase distributions in each branch. However, it is difficult to orient the orifice perfectly and as a result the refrigerant will exit the orifice in direction that is not along the centerline of the distributor. In addition, gravity effects will affect the flow and phase distributions when the distributor is oriented horizontally. However, the impact of these imperfections can be reduced through proper design of the base of the distributor.

The flow through a refrigerant flow distributor involves complicated phenomena of phase separation and distribution. If the flow were fully mixed and the volume fractions of each phase were the same everywhere, then the flow would be homogeneous and could be modeled as a single-phase problem. However, the volume fractions of each are usually not uniform inside the flow distributor and multiphase models are necessary to simulate the phase distribution and separation phenomena. Several CFD codes have been successfully used to predict void fraction profiles in phase separation and phase distribution applications. However, they have been primarily applied to two-dimensional geometries with air-water mixtures. There appears to be no application of CFD modeling to refrigerant distributors in the literature.

Boisson and Malin (1996) applied PHOENICS to predict two-phase flow in bubble columns. An inter-phase slip algorithm (IPSA) was incorporated with the interfacial lift, drag and virtual mass forces in this two-fluid model. The predictions were compared with the measured circulation patterns and void fraction distributions. It

was shown that the model can predict void fraction peaking near the wall for an air-water upflow case and void coring (i.e., void fraction concentration near the pipe's centerline) for a bubbly column case. The interfacial lift and virtual mass forces were believed to cause these lateral phase distribution profiles. Class et al. (1991) and Liu (1991) pointed out that the bubble size effects are also very important. The importance of bubble size on lateral void phase distribution has also been recognized by other investigators, including Sekoguchi et al. (1982). Moreover, Monji et al. (1991) found that for bubbly air-water upflows, small bubbles tend to be uniformly distributed across the conduits, while large bubbles tend to core, and only the intermediate size bubbles concentrate near the wall of the conduit. Lahey et al. (1993) investigated the phase distribution in complex geometry conduits such as triangular and rectangular pipes and found the void coring and peaking phenomena occurred as well.

Lahey (1990) investigated air-water flow through Tee and Wye junctions and observed the phase separation phenomena. It was explained that the vapor phase has far less axial inertia than the liquid phase, thus the vapor can be expected to more easily turn the corner into the side branch.

FLUENT is a CFD package that is widely used in industry and academia. However, FLUENT 5.5 (latest version at the time of this study) does not include interfacial lift forces. Although PHOENICS has been applied to two-phase flows, it is more difficult to use and it's not clear that it is necessary to consider interfacial lift forces for flow conditions encountered in refrigerant distributors. One of the goals of the current work was to compare predictions of PHOENICS and FLUENT to data available in the literature for air and water mixtures. This allowed general model validation. Since detailed flow and phase distribution data are not available for refrigerant distributors, comparisons between FLUENT and PHOENICS were performed for this application in order to highlight any differences. The goal was to identify an appropriate model for the refrigerant distributors that could be used to develop improved designs.

CFD Modeling

Due to the complexity involved in two-phase flow modeling, most analytical models available in the literature have been developed primarily for one-dimensional phenomena (Peixoto, 1994; Fiorelli, 1999). The most sophisticated of these models are based on a two-fluid modeling approach. The two-fluid modeling approach has been extended to multidimensional flows (Lahey, 1990) and has been adopted by several state-of-the-art multi-dimensional computer codes (e.g. PHOENICS, TRAC and RELAP5). Throughout the current study, an adiabatic flow was assumed with no phase change. A description of the basic modeling approaches considered in this study follows.

Multi-Phase Mass and Momentum Equations

In the absence of phase change within the domain, conservation of mass for each phase leads to

$$\frac{\partial}{\partial t}\left(\rho_i \alpha_i\right) + div\left(\rho_i \alpha_i \vec{V}_i\right) = 0 \tag{1}$$

where for phase i, α_i is the volume fraction, $\vec{V}_i$ is the velocity vector, and ρ_i is the density.

For each phase, the momentum conservation equation is:

$$\frac{\partial}{\partial t}\left(\rho_i \alpha_i u_{il}\right) + div\left(\rho_i \alpha_i \vec{V}_i u_{il}\right) = \alpha_i\left(-\vec{l}\cdot\nabla P + B_{il}\right) + F_{il} + I_{il} \tag{2}$$

where P is pressure, which is the same for each phase; $\vec{l}$ is a unit vector in the l-direction; u_{il} is velocity of phase i in direction l; B_{il} is the l-direction body force per unit volume of phase i; F_{il} is the friction force exerted on phase i by stresses within that phase; and I_{il} is the momentum transfer to phase i resulting from interaction with other phases occupying the same cell. For steady-state problems, the time-dependent terms disappear in the mass conservation and momentum conservation equations. For $\alpha_i = 1$, the equations are applicable to single-phase flow problems. In this case, the I_{il} term vanishes from the momentum equation.

Two-Phase Models in FLUENT 5.5 (VOF & ASM Models)

There are two approaches for handling multi-phase flows in FLUENT 5.5. In the volume of fluid (VOF) formulation, the different phases assume the same local velocity and pressure, and properties represent volume-averaged values determined from the local volume fraction of each of the phases. The densities of the individual phases are assumed to be constant and only a single mass conservation is applied to the vapor phase, such that equation 1 reduces to

$$\frac{\partial}{\partial t}(\alpha_g) + div(\alpha_g \vec{V}) = 0 \tag{3}$$

where α_g is the void fraction of the vapor phase. The local void fraction of the liquid phase is determined from the constraint that the sum of the individual void fractions is unity.

For volume-averaged properties, equation 2 reduces to

$$\frac{\partial}{\partial t}(\rho u_l) + div(\rho \vec{V} u_l) = \left(-\vec{l} \cdot \nabla P + B_l \right) + F_l \tag{4}$$

where F_l is friction force per unit volume exerted by stresses within that location. The average properties of density, ρ, and viscosity, μ, are determined from the volume fractions of all phases. Since only a single momentum equation is solved, there are no interfacial forces between phases that are considered in the VOF model.

The algebraic slip mixture (ASM) model allows for different local velocities and properties of the phases through the use of an algebraic model that relates phase velocities. An overall mass conservation equation for the ASM model is

$$\frac{\partial}{\partial t}(\rho_m) + div(\rho_m \vec{V}) = 0 \tag{5}$$

where $\rho_m = \sum_{i=1}^{2} (\alpha_i \rho_i)$. Again, the local void fractions must sum to unity.

The momentum equation for the mixture is

$$\sum_{i=1}^{2} \left[\frac{\partial}{\partial t}(\rho_i \alpha_i u_{il}) + div(\rho_i \alpha_i \vec{V}_i u_{il}) \right] = -\vec{l} \cdot \nabla P + \sum_{i=1}^{2} \left[\alpha_i B_{il} + F_{il} + div(\alpha_i \rho_i \vec{V}_{Di}) \right] \tag{6}$$

where $\vec{V}_{Di}$ is the drift velocity for phase i and is given by

$$\vec{V}_{Di} = \vec{V}_i - \vec{V}_m \tag{7}$$

and where

$$\vec{V}_m = \sum_{i=1}^{2} \left(\frac{\alpha_i \rho_i \vec{V}_i}{\rho_m} \right) \tag{8}$$

The relative velocity (also referred to as the slip velocity) is defined as the velocity of the secondary phase (vapor) relative to the primary-phase (liquid) velocity or

$$\vec{V}_{1,2} = \vec{V}_2 - \vec{V}_1 \tag{9}$$

In the ASM model, the relative velocity is estimated as

$$\vec{V}_{1,2} = \tau_{2,1} \vec{a} \tag{10}$$

where $\vec{a}$ is the secondary phase particle's acceleration and $\tau_{2,1}$ is the particulate relaxation time. The particle acceleration is determined from the solution for the velocity field, whereas the relaxation time is calculated as

$$\tau_{2,1} = \frac{\rho_2 d_2^2}{18 \mu_1} \tag{11}$$

where d_2 and μ_1 are secondary phase particle diameter and primary phase dynamic viscosity, respectively. The user specifies the particle diameter based upon an understanding of the flow geometry.

Although the ASM model allows velocity slip between phases, only one set of momentum equations for the mixture is solved and an additional force term related to the slip velocity is added to the equation.

Two-Phase Modeling in PHOENICS (IPSA)

The inter-phase slip algorithm (IPSA) incorporated in PHOENICS employs individual momentum equations for each phase with interfacial lift and virtual mass forces. Equations 1 and 3 are applied with the virtual mass and interfacial lift forces added into the term I_{il}, such that

$$I_{il} = M_{vm} + M_{lft} \tag{12}$$

where M_{vm} and M_{lft} are virtual mass and interfacial forces, respectively. The lift forces act on a particle mainly due to velocity gradients in the primary-phase flow field. The lift force will be more significant for larger particles. Thus, the inclusion of lift forces is not appropriate for closely packed particles or for very small particles. The "virtual mass effect" occurs when a secondary phase accelerates relative to the primary phase. The inertia of the primary-phase mass encountered by the accelerating particles (or droplets or bubbles) exerts a "virtual mass force" on the particles. The virtual mass effect is significant when the secondary phase density is much smaller than the primary phase density (e.g., for air and water in a bubble column). The interfacial forces are estimated using empirical relations.

Turbulence Modeling

Both FLUENT and PHOENICS incorporate the $k-\varepsilon$ model for turbulence. The friction force F_{il} involves the quantities of turbulent fluctuation velocities with the form of $\overline{u}_{il}^{'}\overline{u}_{im}^{'}$, where $\overline{u}_{il}^{'}$ and $\overline{u}_{im}^{'}$ are turbulent fluctuation velocity components of u_{il} and u_{im}, respectively. According to Boussinesq's assumption (employed in the $k-\varepsilon$ model), it may be expressed as:

$$\overline{u}_{il}^{'}\overline{u}_{im}^{'} = \mu_t\left(\frac{\partial u_{il}}{\partial x_m} + \frac{\partial u_{im}}{\partial x_l}\right) - \frac{2}{3}\delta_{ij}k \tag{13}$$

where $k = \frac{1}{2}\left(\overline{u}_{il}^{'}\overline{u}_{im}^{'}\right)$ is the turbulent kinetic energy, δ_{ij} is 1 for $i=j$ and 0 otherwise, and μ_t is the turbulent viscosity (eddy viscosity) which is related to k and to the rate of dissipation ε by:

$$\mu_t = C_\mu \frac{k^2}{\varepsilon} \tag{14}$$

C_μ is a model constant with a value of 0.09 in the $k-\varepsilon$ model.

The eddy viscosity together with molecular viscosity gives an effective viscosity:

$$\mu_{eff} = \mu + \mu_t \tag{15}$$

The standard $k-\varepsilon$ model is a two-equation turbulent model, which means both k and ε are solved from transport equations:

$$\frac{\partial}{\partial x_{il}}\left(\rho u_{il} k\right) = \frac{\partial}{\partial x_{il}}\left(\frac{\mu_t}{\sigma_k}\frac{\partial k}{\partial x_{il}}\right) + G_k + G_b - \rho\varepsilon \tag{16}$$

$$\frac{\partial}{\partial x_{il}}\left(\rho u_{il} \varepsilon\right) = \frac{\partial}{\partial x_{il}}\left(\frac{\mu_t}{\sigma_k}\frac{\partial \varepsilon}{\partial x_{il}}\right) + C_{1\varepsilon}\frac{\varepsilon}{k}G_k - C_{2\varepsilon}\rho\frac{\varepsilon^2}{k} \tag{17}$$

$C_{1\varepsilon}$, $C_{2\varepsilon}$, σ_k and σ_ε are model constants with values given in Table 1:

G_k is calculated from:

$$G_k = \mu_t \left(\frac{\partial u_{il}}{\partial x_{im}} + \frac{\partial u_{im}}{\partial x_{il}} \right) \frac{\partial u_{il}}{\partial x_{im}} \tag{18}$$

Boundary Conditions

All the geometries simulated in this paper had an inflow boundary, outflow boundaries, solid walls and in some cases, a symmetry plane. The inflow boundary had specified inlet velocity with uniform void fractions. Constant and uniform pressures were specified for all outflow boundaries. Although laminar transport is considered in the $k-\varepsilon$ model, it is not applicable near walls where the turbulence Reynolds number is low. In these regions, equilibrium wall functions are used in boundary conditions, which are specified at a point located in the fully turbulent regime. At this location, the logarithmic law of the wall prevails and the turbulence is assumed to be in local equilibrium.

Model Comparisons

As a first step in evaluating the applicability of CFD to two-phase flow in refrigerant distributors, results of predictions from FLUENT and PHOENICS were compared with experimental results available in the literature. These data are for air and liquid water mixtures having relatively low inlet velocities (less than 10 m/s). In refrigerant distributors, the velocities exiting the orifice and entering the distributor are much higher (up to 50 m/s) and the difference in densities between the two phases is much smaller. Modeling of the flow and phase distributions for the air-water cases is more difficult and therefore the data for these flow geometries allow general model validation. Detailed flow and phase distribution data are not available for refrigerant distributors. However, results from FLUENT and PHOENICS were compared with each other for this application in order to highlight any differences for this case. The goal was to identify an appropriate model for the refrigerant distributors that could be used to develop improved designs.

For all the simulations done in both FLUENT and PHOENICS, a no-slip condition was assumed between the two phases at the inlet of the computational domain and the standard k-ε model was employed as the turbulence model.

Air-water Turbulent Pipe Flow

Experimental measurements for the mean radial profiles of void fraction are available in the open literature (Seriwaza et al., 1992) for turbulent air-water up flow in a pipe. The Reynolds number based on the superficial liquid velocity and the pipe diameter was 80,000. The inlet superficial gas and liquid velocities were $j_g = u_g \times \alpha = 0.077$ m/s and $j_l = u_l \times (1-\alpha) = 1.36$ m/s, where u_g, u_l and α are gas velocity, liquid velocity and void fraction, respectively.

For simulations using FLUENT and PHOENICS, two-dimensional, axisymmetric calculations were performed with a computational domain extending 35 pipe diameters downstream, corresponding to the experimental measuring station that lies in the region of fully developed flow.

Figure 2 shows comparisons between measurements and FLUENT predictions (both VOF and ASM models) of local void fraction as a function of radial position from the center (r) for one vertical location within the pipe. The data show void peaking near the wall, whereas the predicted void fraction is nearly uniform throughout the pipe cross-section. The VOF model does not consider velocity slip, so a straight pipe with a homogeneous two-phase inlet will have a uniform void fraction distribution in the flow field. The velocity slip scheme in the ASM model has the potential of changing the void fraction profile inside the computational domain. However, there are no radial forces such as the interfacial lift force and the resulting void fraction profile is also uniform.

Figure 3 shows comparisons between measurements and PHOENICS predictions of void fraction. In this case, profiles of void fraction and liquid velocity are in good agreement with the experimental data (r/R is the non-dimensional radial position within the pipe). The void fraction peaks at the wall, indicating that the gas bubbles have been driven to the wall by the interfacial lift and virtual mass forces that are incorporated in the IPSA model. The wavy behavior of the void fraction distribution near the pipe wall in the simulations does not appear to be due to numerical problems. The grid size was reduced with no effect on the results. In addition, the predicted velocity profile did not exhibit this waviness. The wavy behavior could be real, since there is not enough resolution in the data to capture this effect.

Phase Separation in a Tee Junction

There have been a number of published studies concerned with air-water phase separation in Tee branching pipes (Collier, 1975; Honan and Lahey 1981; Zetzmann, 1982). Figure 4 shows the flow configuration in a Tee junction, where w and x represent the mass flow rate and quality, respectively.

The experimental data in the literature for this problem show that over a wide range of mass extraction ratios (the ratio of the mass flow rate at the exit of the branch pipe to the mass flow rate at the inlet pipe; i.e. w_3/w_1) almost complete phase separation occurred (i.e., $w_3x_3=w_1x_1$). Vapor primarily goes to the side branch and liquid mainly goes to the straight run. The trends observed in the experiments are attributable to the fact that the vapor phase normally has a smaller axial momentum than the liquid phase (i.e. $\rho_g u_g^2 << \rho_l u_l^2$). Therefore, the vapor more easily turns into the side branch. The Tee junction case studied by Honan and Lahey (1981) was chosen to be simulated in both FLUENT and PHOENICS. The diameters of the inlet and branch pipes were both equal to 0.038 m. The superficial velocity inlet conditions for the case considered were $j_g = 10\, m/s$ and $j_l = 1\, m/s$.

Both the VOF and ASM models were employed in FLUENT to predict flow and phase distributions through the Tee junction. Figure 5 gives the ratio of branch exit to inlet quality (x_3/x_1) as a function of the ratio of the branch exit to inlet mass flow rate (w_3/w_1) for the experiments and model predictions. For x_3/x_1 equal to 1, the flow is homogeneous and the void fraction is uniform throughout. Both FLUENT models predict a uniform void fraction, independent of the flow rate ratio. In the actual case, there is a significant flow separation and the quality within the branch is much higher than the inlet quality. Furthermore, there is a flow rate ratio that leads to maximum phase separation. For the VOF model, a uniform void fraction distribution results from the lack of a velocity slip and the homogeneous two-phase inlet. For the ASM model, the slip velocity effects were not large enough to change the void fraction distribution within the branch.

Lahey (1990) used PHOENICS with the measured inlet void fraction profile to predict the phase separation phenomena in two-phase flow through the Tee. Figure 6 shows comparisons between the data and the PHOENICS predictions. The agreement is excellent.

Refrigerant Flow Distribution

Interfacial lift and virtual mass forces are important elements in predicting phase separation and phase distribution phenomena for air-water mixtures at the velocities considered in the literature. However, refrigerant distributors operate with higher inlet velocities and refrigerant vapor and liquid properties are much different than those of air and water. As a result, FLUENT may provide accurate predictions of phase separation and distribution for refrigerant distributors. Since PHOENICS has been validated for several flow geometries involving air-water mixtures, it provides a baseline for evaluating predictions associated with FLUENT.

In order to evaluate the application of FLUENT for modeling refrigerant distributors, a 2-dimensional simulation of the simple distributor geometry shown in Figure 7 was developed. The geometry and inlet boundary conditions were chosen to be representative of a commercially available distributor with an orifice at the inlet. The properties of the two phases were calculated from properties of R-22 at 5^0C. Gravity was not considered. The orifice was assumed to be tipped slightly in the y direction to simulate manufacturing imperfections and create an uneven flow distribution. The x and y components of the refrigerant velocities at the inlet were $u_x = 50.79$ m/s and $u_y = 3$ m/s. The ASM model in FLUENT was employed.

Table 1 gives comparisons between PHOENICS and FLUENT predictions of outlet flow rates and qualities. The predictions of branch liquid and vapor flow rates were very similar for the two codes. Figures 8 – 12 give velocity fields and void fraction contours for the two codes. For this flow geometry, the phase distributions and velocity fields are very similar for FLUENT and PHOENICS predictions. It appears that interfacial lift and virtual mass forces are negligible for this high momentum two-phase flow.

Conclusions

FLUENT 5.5 failed to predict experimental data available in the literature for two-phase flow distribution and separation with air and liquid water having relatively low inlet stream momentum. On the other hand, PHOENICS predictions were in close agreement with the measurements in all cases. The IPSA (inter-phase slip algorithm) model in PHOENICS solves continuity and momentum equations for each phase and incorporates interfacial lift and virtual mass forces that are not present in FLUENT 5.5. However, these forces do not appear to be important for the high momentum inlet flows encountered in refrigerant distributors. For a typical distributor geometry, predictions of two-phase distribution and separation were quite similar for FLUENT 5.5 and

PHOENICS. As a result, FLUENT is applicable for studying improved refrigerant distributor designs and was used for this purpose as described in a companion paper by Li et. al. (2002).

References

N. Boisson and M.R. Malin, Numerical prediction of two-phase flow in bubble columns, Int. J. for numerical methods in fluids (1996) Vol. 23, 1289-1310.

G. Class, R. Meyder, W. Sengpiel, Measurement of spatial gas distribution and turbulence structure in developing bubbly two-phase in vertical channels, Proceedings of the International Conference on Multiphase Flows '91-Tsububa 1 (1991) pp. 473-477.

J. Collier, Single-Phase and two-phase flow behavior in primary circuit components, symposium on two-phase flow and heat transfer in water cooled nuclear reactors, Dartmouth University (1975).

F. A. S. Fiorelli, R. A. Peixoto, M. A. S. Paiva, O. M. Silvares, Numerical study on refrigerant mixtures flow in capillary tubes, 1998 International Refrigeration Conference at Purdue, (1998).

T. J. Honan & R. T Lahey, Jr., The measurement of phase separation in wyes and Tees, Nuclear Eng. & Design Vol. 54, No. 1, (1981) pp.93-102.

R. T. Lahey, Jr., The analysis of phase separation phenomena in branch conduits, Dynamics of two-phase flow (1990) pp.313-346.

R. T. Lahey, Jr., M. Lopez de Bertodano and O.C. Jones, Phase distribution in complex geometry ducts, Nucl. Eng. Design 141 (1993) pp. 177-201.

G. Li, J.E. Braun, E.A. Groll, S. Frankel, Z. Wang, Evaluating the Performance of Refrigerant Flow Distributors, 2002 International Refrigeration Conference at Purdue, (2002).

T. J. Liu, the effect of bubble size on void fraction distribution in a vertical channel, Proceedings of the International Conference on Multiphase Flows '91-Tsububa 1 (1991) pp. 453-457.

H. Monji, G. Matsui, Effect of bubble size on the structure of vertical bubble flow, Proceeding s of the International Conference on Multiphase Flow '91-Tsububa 1 (1991) pp. 449-452.

R. A. Peixoto, C. W. Bullard, A simulation and design model for capillary tube-suction line heat exchangers, 1994 International Refrigeration Conference at Purdue, (1994).

K. Sekoguchi, T. Sato and T. Honda, Two-phase flow in vertical noncircular channels, Int. J. Multiphase Flow 8(6) (1982) pp. 641-655.

A. Serizawa, I. Kataoka and I. Michiyoshi, Phase distribution in bubbly flow: Data Set No. 24, Multiphase Science and Technology, Vol. 6. Hemisphere, Washington DC. (1992) P. 257.

K. Zetzmann, Phasenseparation und Druckabfall in Zweiphasig Durchstroemten Vertikalen Rohrabzweigungen, Doctorate Thesis, University of Hanover, FRG, (1982).

Table 1 Constant values employed in $k-\varepsilon$ turbulence model

Constant	C_μ	σ_k	σ_ε	$C_{1\varepsilon}$	$C_{2\varepsilon}$
Value	0.09	1	1.3	1.44	1.92

Table 2: Branch flow rates & qualities from PHOENICS and FLUENT for 2-D refrigerant distributor

	PHOENICS			FLUENT		
	mass flow rate (kg/s)			mass flow rate (kg/s)		
	vapor	liquid	quality	vapor	liquid	quality
Outlet 1	2.61	13.57	0.1613	2.70	14.05	0.161
Outlet 2	1.163	6.025	0.1618	1.07	5.55	0.161

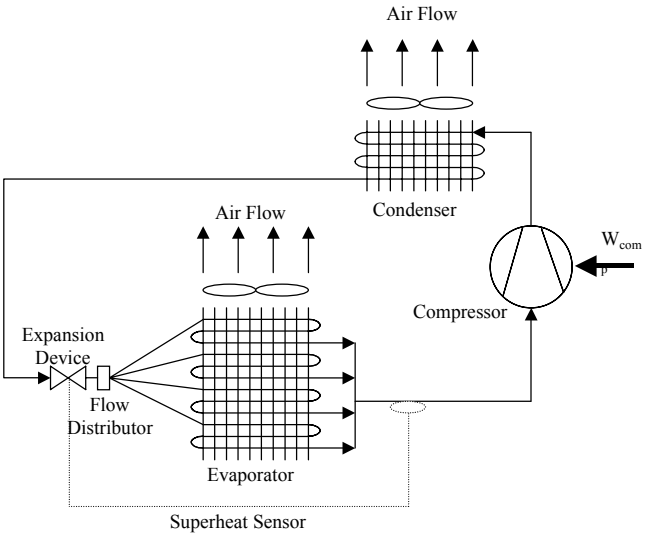

Figure 1: Vapor compression cycle with refrigerant distributor

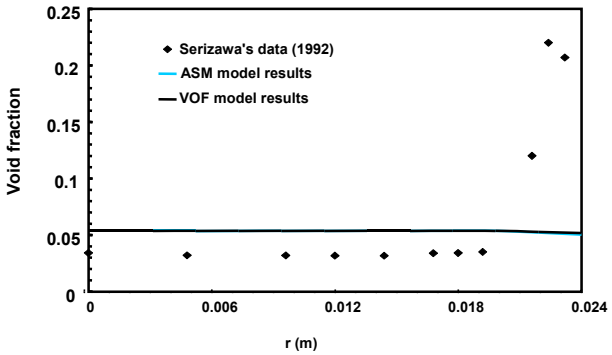

Figure 2: FLUENT prediction and measured void fraction profiles for Seriwaza's (1992) bubbly column case

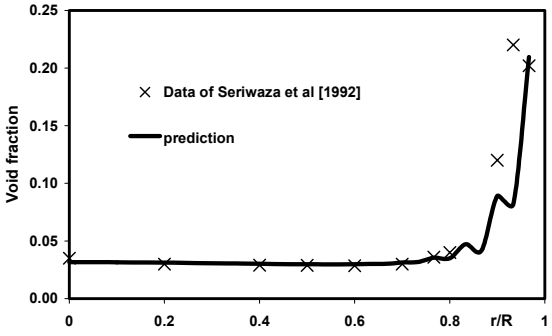

Figure 3: Comparison between PHOENICS predictions and measurements for void fraction radial profiles for Seriwaza's (1992) bubbly column.

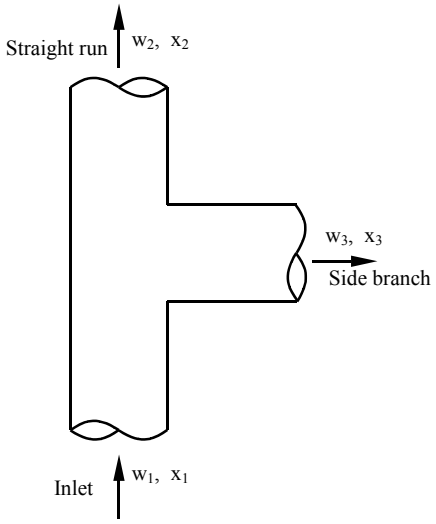

Figure 4: Flow configurations in a Tee junction

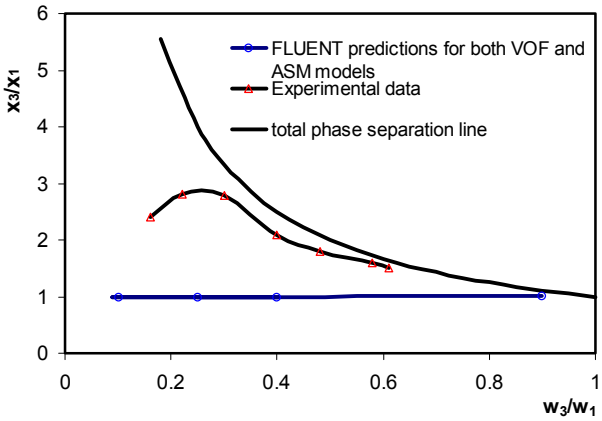

Figure 5: Comparison of experimental and FLUENT predictions for phase distribution in a Tee junction (data from Lahey (1990))

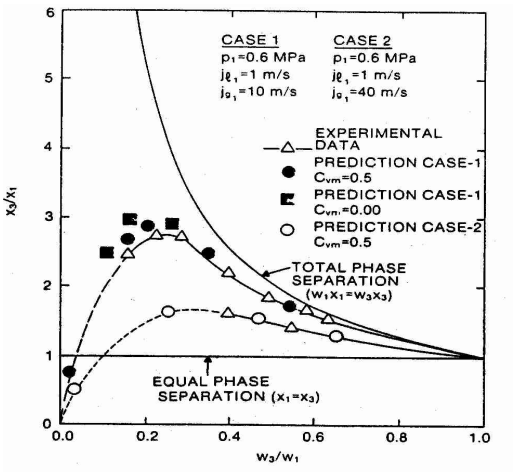

Figure 6: Comparison of experimental and PHOENICS predictions for phase distribution in a Tee junction (from Lahey (1990)).

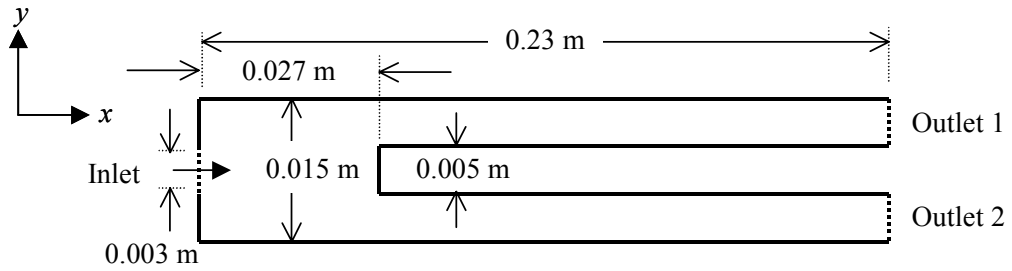

Figure 7. Geometry of the 2-D refrigerant distributor

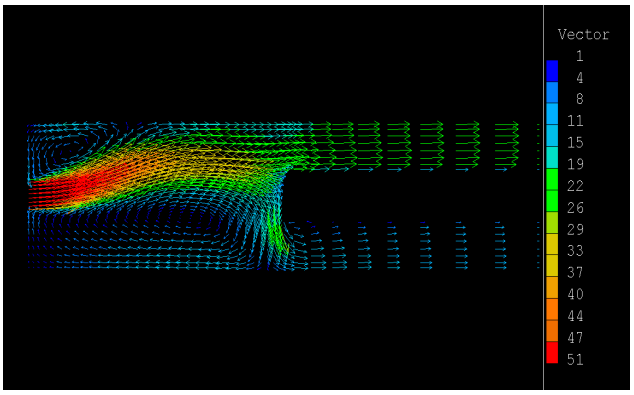

Figure 8: PHOENICS prediction of velocity field for 2-dimensional refrigerant distributor

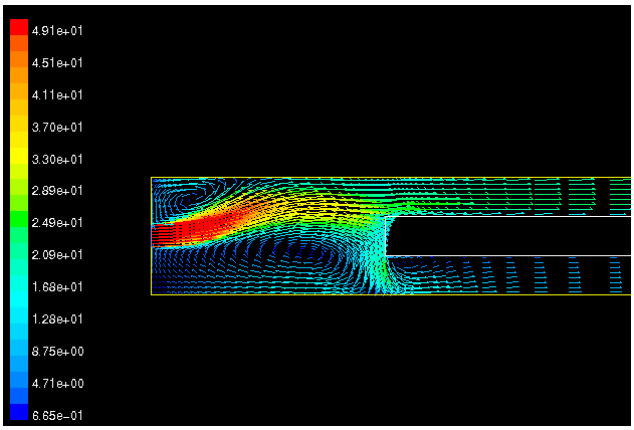

Figure 9: FLUENT prediction of velocity field for 2-dimensional refrigerant distributor

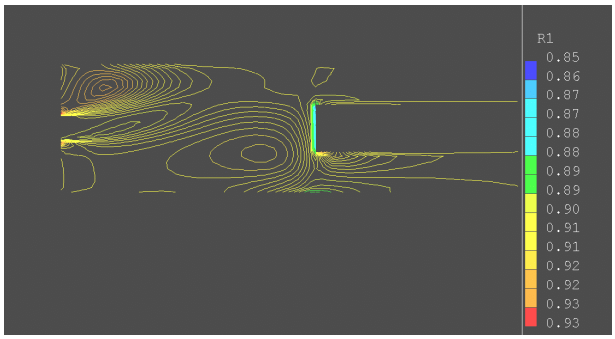

Figure 10: PHOENICS prediction of void fraction contour for 2-dimensional refrigerant distributor

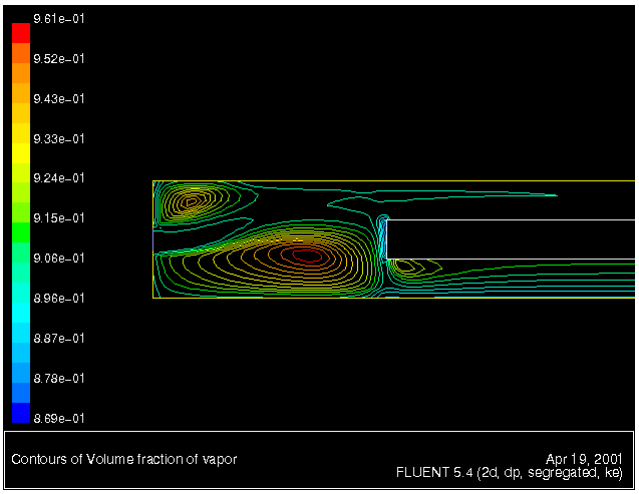

Figure 11: FLUENT prediction of void fraction contour for 2-dimensional refrigerant distributor